PROCEEDINGS
OF THE ROYAL SOCIETY A
MATHEMATICAL, PHYSICAL AND ENGINEERING SCIENCES

rspa.royalsocietypublishing.org

Research

Article submitted to journal

Subject Areas:
mathematical modelling

Keywords:
advection, Taylor–Aris dispersion, rivulet

Author for correspondence:
S. K. Wilson
e-mail: s.k.wilson@strath.ac.uk

Advection and Taylor–Aris dispersion in rivulet flow

F. H. H. Al Mukahal[1,2], B. R. Duffy[1] and S. K. Wilson[1]

[1]Department of Mathematics and Statistics, University of Strathclyde, Livingstone Tower, 26 Richmond Street, Glasgow G1 1XH, United Kingdom
[2]Department of Mathematics and Statistics, King Faisal University, P.O. Box 400, Hafouf 31982, Kingdom of Saudi Arabia

Motivated by the need for a better understanding of the transport of solutes in microfluidic flows with free surfaces, the advection and dispersion of a passive solute in steady unidirectional flow of a thin uniform rivulet on an inclined planar substrate driven by gravity and/or a uniform longitudinal surface shear stress are analysed. Firstly, we describe the short-time advection of both an initially semi-infinite and an initially finite slug of solute of uniform concentration. Secondly, we describe the long-time Taylor–Aris dispersion of an initially finite slug of solute. In particular, we obtain the general expression for the effective diffusivity for Taylor–Aris dispersion in such a rivulet, and discuss in detail its different interpretations in the special case of a rivulet on a vertical substrate.

1. Introduction

One of the ongoing challenges in microfluidics is that of controlling and optimising the transport (*i.e.* the mixing and dispersion) of solutes at small length scales and low Reynolds numbers (see, for example, the reviews by Stone, Stroock and Ajdari [1], Darhuber and Troian [2], and Lee *et al.* [3]). The dispersion (*i.e.* the combined effect of advection and diffusion) of a solute in a steadily flowing fluid is a classical problem in fluid mechanics which arises in numerous practical situations (such as, for example, the spread of pollutants in rivers, chromatographic separation, and the transport of dissolved drugs in the bloodstream) and has been the subject of a huge body of theoretical and experimental research, the vast majority of it originating from the pioneering papers by Taylor [4,5] and Aris

THE ROYAL SOCIETY
PUBLISHING

[6] published in this journal. The key insight of this pioneering work was that after a sufficiently long time the mean concentration of solute adopts a symmetric Gaussian distribution which moves downstream with the mean speed of the flow and spreads in the flow direction with an effective (or enhanced) diffusion coefficient, $D_{\rm eff}$, which is larger than the molecular diffusion coefficient, D, due to the presence of the flow. This phenomenon is now known as Taylor–Aris (or sometimes simply just Taylor) dispersion. In the simplest case of Poiseuille flow in a pipe of circular cross-section with diameter d, Taylor [4] obtained the famous expression $D_{\rm eff} = D(1 + {\rm Pe}_{\rm con}^2/192)$, where ${\rm Pe}_{\rm con} = \overline{u}d/D$ is the conventional Péclet number based on the mean velocity over the cross-section of the pipe, $\overline{u}$. As Witelski and Bowen [7, Chap. 11] say, "Taylor's original paper was presented in his unique and very physically intuitive style; it is deceptively short and challenging to follow", and subsequently many authors have sought to formalise Taylor's argument using a variety of methods, including the method of moments (Aris [6]), Fourier series (Lungu and Moffatt [8]), the method of multiple scales (Pagitsas, Nadim and Brenner [9], Zhang and Frigaard [10]), centre-manifold theory (Mercer and Roberts [11], Young and Jones [12], Balakotaiah and Chang [13]), and Liapunov–Schmidt reduction (Ratnakar and Balakotaiah [14]). There is now an extensive literature on dispersion in channels with a variety of cross-sectional shapes (see, for example, Brenner and Edwards [15], Dutta and Leighton [16], Dutta, Ramachandran and Leighton [17], and Dutta [18]), and, in particular, a body of work on dispersion in wide channels (see, for example, Doshi, Daiya and Gill [19], Chatwin and Sullivan [20], Pagitsas, Nadim and Brenner [9], Guell, Cox and Brenner [21], Smith [22,23], and Ajdari, Bontoux and Stone [24]). However, with the notable exception of the work of Darhuber *et al.* [25] on mixing in thermocapillary flows on micropatterned surfaces, there has been surprisingly little theoretical work on transport of solutes in microfluidic flows with free surfaces and, in particular, on the topic of the present contribution, namely the dispersion of a passive solute in a rivulet flow. While the present work is primarily motivated by and described in the context of the dispersion of a solute, the present results also apply to the transport of heat with insulating boundary conditions and can readily be extended to other thermal boundary conditions (see, for example, Lungu and Moffatt [8]), and so the present work is also relevant to the wide range of practical situations involving heat transfer in the presence of rivulets (see, for example, Kabov [26] and Kabov, Bartashevich and Cheverda [27]).

In addition to in microfluidics, rivulets of many different fluids occur in a wide variety of other practical contexts, including heat exchangers, trickle-bed reactors and various coating processes, and as a result there has been considerable theoretical work on locally unidirectional rivulet flow (see, for example, Paterson, Wilson and Duffy [28] and the references therein). In particular, Young and Davis [29], Duffy and Moffatt [30], Myers, Liang and Wetton [31], Saber and El-Genk [32], Wilson and Duffy [33], Sullivan, Wilson and Duffy [34], Benilov [35], Tanasijczuk, Perazzo and Gratton [36], Wilson, Sullivan and Duffy [37], and Herrada *et al.* [38] considered various aspects of locally unidirectional rivulet flow and its stability.

In the present contribution we analyse advection and dispersion of a passive solute in steady unidirectional flow of a thin uniform rivulet on an inclined planar substrate driven by gravity and/or a uniform longitudinal surface shear stress. In particular, we obtain the general expression for the effective diffusivity $D_{\rm eff}$ for Taylor–Aris dispersion in such a rivulet, and discuss in detail its different interpretations in the special case of a rivulet on a vertical substrate.

2. Rivulet flow

Consider steady unidirectional flow of a thin uniform rivulet of incompressible Newtonian fluid on a planar substrate inclined at an angle α ($0 \leq \alpha \leq \pi$) to the horizontal, the flow being driven by gravity and/or a uniform longitudinal surface shear stress τ. Aspects of this flow problem were described by Wilson and Duffy [33] and Sullivan [34]; here we present only the key results relevant to the present study of advection and Taylor–Aris dispersion of a passive solute in such a flow.

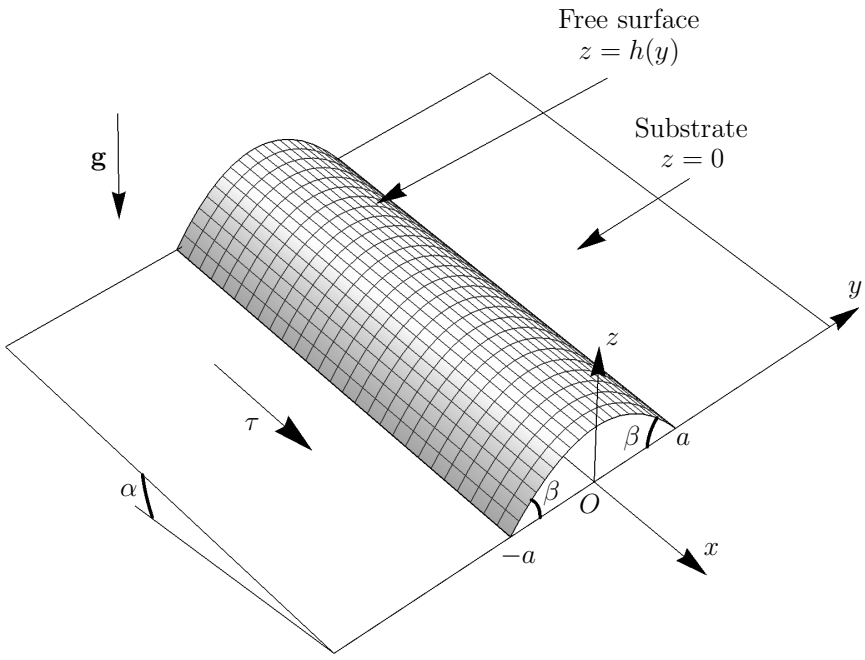

Figure 1. Sketch of the geometry of the problem: steady unidirectional flow of a thin uniform rivulet of incompressible Newtonian fluid on a planar substrate inclined at an angle α ($0 \leq \alpha \leq \pi$) to the horizontal and subject to a uniform longitudinal surface shear stress τ.

Referred to a Cartesian coordinate system $Oxyz$ with Ox down the line of greatest slope and Oz normal to the substrate at $z = 0$, as shown in Fig. 1, we scale and nondimensionalise variables according to

$$\begin{gathered} y = \ell y^*, \qquad z = \epsilon \ell z^*, \qquad a = \ell a^*, \qquad h = \epsilon \ell h^*, \qquad \beta = \epsilon \beta^*, \qquad A = \epsilon \ell^2 A^*, \\ u = U u^*, \qquad p = p_{\mathrm{a}} + \epsilon \rho g \ell p^*, \qquad \tau = \epsilon \rho g \ell \tau^*, \qquad Q = \epsilon U \ell^2 Q^*, \qquad \overline{u} = U \overline{u}^*, \end{gathered} \tag{2.1}$$

where $\mathbf{u} = u(y, z)\mathbf{i}$ and p are the fluid velocity and pressure, $\ell = (\gamma/\rho g)^{1/2}$ is the capillary length, $z = h(y)$ denotes the free surface of the rivulet, ϵ ($\ll 1$) is the aspect ratio of the cross-section of the rivulet, a and A are the semi-width and cross-sectional area of the rivulet, β denotes the contact angle, μ and ρ are the constant viscosity and density of the fluid, $U = \epsilon^2 \rho g \ell^2/\mu$ is the velocity scale associated with gravity-driven flow, g is gravitational acceleration, Q is the volume flux of fluid down the rivulet, $\overline{u}$ is the mean velocity over the cross-section, γ is the coefficient of surface tension, and p_{a} is atmospheric pressure. Then, with the superscript stars dropped for clarity, the governing Navier–Stokes equation gives, at leading order in ϵ,

$$u_{zz} = -\sin\alpha, \qquad p_y = 0, \qquad p_z = -\cos\alpha, \tag{2.2}$$

which are to be integrated subject to the boundary conditions

$$u = 0 \quad \text{on} \quad z = 0, \qquad u_z = \tau \quad \text{and} \quad p = -h'' \quad \text{on} \quad z = h, \tag{2.3}$$

where a prime denotes differentiation with respect to argument. Thus

$$p = (h - z)\cos\alpha - h'', \qquad u = \frac{\sin\alpha\left(2hz - z^2\right)}{2} + \tau z, \tag{2.4}$$

in which h satisfies

$$(h'' - h\cos\alpha)' = 0, \tag{2.5}$$

to be integrated subject to the contact-line conditions

$$h = 0, \quad h' = \mp\beta \quad \text{at} \quad y = \pm a. \tag{2.6}$$

Therefore

$$Q = \int_{-a}^{a}\int_{0}^{h} u\,\mathrm{d}z\,\mathrm{d}y = \frac{\sin\alpha\, I_3}{3} + \frac{\tau I_2}{2}, \qquad \overline{u} = \frac{Q}{A} = \frac{\sin\alpha\, I_3}{3I_1} + \frac{\tau I_2}{2I_1}, \tag{2.7}$$

where we have defined I_1 $(= A)$, I_2 and I_3 by

$$I_n = \int_{-a}^{a} h^n\,\mathrm{d}y \qquad (n = 1, 2, 3). \tag{2.8}$$

In Appendix A we provide the solution of equations (2.5)–(2.6) for h, as well as explicit expressions for the quantities I_1, I_2 and I_3 defined in (2.8) and appearing in the expressions for Q and $\overline{u}$ given in (2.7). In general, for given values of α and τ, any two of the four quantities a, β, Q and the maximum thickness $h_\mathrm{m} = h(0)$ may be prescribed. (In practice, it is difficult to prescribe h_m and so, for brevity, we will not consider this situation further in the present work.)

The maximum and minimum fluid velocities over the rivulet, which we denote by u_max and u_min, respectively, satisfy $u_\mathrm{max} \geq 0$ and $u_\mathrm{min} \leq 0$. When $\tau \geq 0$ (*i.e.* when the surface shear stress acts in the same direction as gravity) the velocity is downwards everywhere (*i.e.* $u \geq 0$ throughout the rivulet), $u_\mathrm{max} = h_\mathrm{m}(h_\mathrm{m}\sin\alpha + 2\tau)/2$ occurs at the apex of the rivulet (*i.e.* at $y = 0$, $z = h_\mathrm{m}$) and $u_\mathrm{min} = 0$ occurs on the substrate $z = 0$, but when $\tau < 0$ (*i.e.* when the surface shear stress opposes gravity) the velocity is upwards (*i.e.* $u < 0$) near the edges of the rivulet, but can be downwards elsewhere. In particular, when $\tau \leq -h_\mathrm{m}\sin\alpha$ the velocity is upwards throughout the rivulet with $u_\mathrm{max} = 0$ and $u_\mathrm{min} = h_\mathrm{m}(h_\mathrm{m}\sin\alpha + 2\tau)/2$ occurring at the apex of the rivulet, but when $-h_\mathrm{m}\sin\alpha < \tau < 0$ there is a region of downwards flow in the centre of the rivulet with $u_\mathrm{max} = (h_\mathrm{m}\sin\alpha + \tau)^2/(2\sin\alpha)$ occurring within this region at $y = 0$, $z = (h_\mathrm{m}\sin\alpha + \tau)/\sin\alpha$ and $u_\mathrm{min} = -\tau^2/(2\sin\alpha)$ occurring on the free surface $z = h$ at the positions at which $h\sin\alpha + \tau = 0$. For future reference note that the flux Q (and hence the mean velocity $\overline{u}$) are positive for $\tau > \tau_\mathrm{c}$, zero for $\tau = \tau_\mathrm{c}$ and negative for $\tau < \tau_\mathrm{c}$, where the critical value $\tau = \tau_\mathrm{c}$ (< 0) corresponding to no net flow is given by $\tau_\mathrm{c} = -2\sin\alpha\, I_3/(3I_2)$. Note that Wilson and Duffy [33] and Sullivan *et al.* [34] give a complete description of the cross-sectional flow patterns in the special cases of a vertical substrate (*i.e.* when $\alpha = \pi/2$) and a perfectly wetting fluid (*i.e.* when $\beta = 0$), respectively.

The special case of purely gravity-driven-flow corresponds simply to $\tau = 0$, in which case the velocity is downwards everywhere with $u_\mathrm{max} = h_\mathrm{m}^2\sin\alpha/2$ and $u_\mathrm{min} = 0$.

On the other hand, the special case of purely surface-shear-stress-driven flow may be obtained by taking the limit $|\tau| \to \infty$ with u rescaled as $u = \tau\widehat{u}$ to give simply $\widehat{u} = z$; then the rescaled flux $\widehat{Q} = Q/\tau$ and the rescaled mean velocity $\widehat{\overline{u}} = \overline{u}/\tau$ satisfy $\widehat{Q} \to I_2/2$ and $\widehat{\overline{u}} \to I_2/(2I_1)$, respectively, and the rescaled minimum and maximum velocities are $\widehat{u}_\mathrm{max} = u_\mathrm{max}/\tau \to h_\mathrm{m}$ and $\widehat{u}_\mathrm{min} = u_\mathrm{min}/\tau \to 0$, again occurring at the apex and on the substrate, respectively.

In the special case of flow on a vertical substrate (*i.e.* when $\alpha = \pi/2$) the solution of equations (2.5)–(2.6) is simply the parabolic profile

$$h = h_\mathrm{m}\left(1 - \frac{y^2}{a^2}\right), \qquad h_\mathrm{m} = \frac{a\beta}{2}, \tag{2.9}$$

so that

$$I_1 = A = \frac{4ah_\mathrm{m}}{3}, \qquad I_2 = \frac{16ah_\mathrm{m}^2}{15}, \qquad I_3 = \frac{32ah_\mathrm{m}^3}{35}, \tag{2.10}$$

and therefore

$$Q = \frac{32ah_\mathrm{m}^3}{105} + \frac{8\tau ah_\mathrm{m}^2}{15}, \qquad \overline{u} = \frac{3Q}{4ah_\mathrm{m}} = \frac{8h_\mathrm{m}^2}{35} + \frac{2\tau h_\mathrm{m}}{5}. \tag{2.11}$$

For future reference, note that in this case when $\tau \geq 0$ then $u_{\max} = a\beta(a\beta + 4\tau)/8$, when $\tau \leq -a\beta/2$ then $u_{\min} = a\beta(a\beta + 4\tau)/8$, and when $-a\beta/2 < \tau < 0$ then $u_{\max} = (a\beta + 2\tau)^2/8$ at $y = 0$, $z = (a\beta + 2\tau)/2$ and $u_{\min} = -\tau^2/2$ at $y = \pm(a(a\beta + 2\tau)/\beta)^{1/2}$, $z = -\tau$, and $\tau_c = -2a\beta/7$.

3. Dispersion of a passive solute in a rivulet

If a passive solute is released into the rivulet then it disperses (that is, it is advected by the flow and diffuses), and its concentration $c = c(x, y, z, t)$, where t denotes time, satisfies the (dimensional) advection–diffusion equation

$$c_t + uc_x = D\left(c_{xx} + \nabla^2 c\right), \tag{3.1}$$

where D is the diffusivity, and ∇^2 denotes the two-dimensional Laplacian given by

$$\nabla^2 = \frac{\partial^2}{\partial y^2} + \frac{\partial^2}{\partial z^2}. \tag{3.2}$$

Also c satisfies the no-flux boundary conditions

$$\mathbf{n} \cdot \nabla c = 0 \quad \text{on} \quad z = 0 \quad \text{and} \quad z = h, \tag{3.3}$$

where $\mathbf{n}$ denotes the unit outward normal to the boundary of the fluid (comprising the substrate and free surface). In addition, we assume that the solute is released at some initial instant $t = 0$ with a prescribed initial distribution $c(x, y, z, 0)$, occupying a (possibly infinite) portion $x_1 \leq x \leq x_2$ of the rivulet, with x_1 and x_2 prescribed.

A key quantity of interest is the mean concentration over the cross-section, which we denote by $\bar{c} = \bar{c}(x, t)$, and which is defined by

$$\bar{c} = \frac{1}{A}\int_{-a}^{a}\int_{0}^{h} c \, \mathrm{d}z \, \mathrm{d}y. \tag{3.4}$$

Also the mean initial concentration over $x_1 \leq x \leq x_2$, which we denote by C_0, is defined by

$$C_0 = \frac{1}{x_2 - x_1}\int_{x_1}^{x_2} \bar{c}(x, 0) \, \mathrm{d}x, \tag{3.5}$$

the integral here being interpreted as an appropriate limit if $x_2 - x_1$ is infinite.

4. Advection of a passive solute in a rivulet

At sufficiently short times after the solute is released, specifically for $t \ll \ell^2/D$, advection dominates over diffusion, and so the effects of diffusion are negligible. In this case the governing equation for c therefore reduces simply to the advection equation $c_t + uc_x = 0$, which has solution $c(x, y, z, t) = c(x - u(y, z)t, y, z, 0)$, reflecting the fact that the particle of solute that is at position $\mathbf{r} = \mathbf{r}_0$ at $t = 0$ is at $\mathbf{r} = \mathbf{r}_0 + ut\mathbf{i}$ at time t. Note that the behaviour of u described in Section 2 immediately implies that when $\tau \geq 0$ all of the solute is advected downwards, when $\tau \leq -h_m \sin\alpha$ all of the solute is advected upwards, and when $-h_m \sin\alpha < \tau < 0$ both downwards and upwards advection occur and, in particular, when $\tau = \tau_c$ the net advection is zero.

We non-dimensionalise and scale variables as in (2.1), together with

$$x = \ell x^*, \qquad t = \frac{\ell}{U}t^*, \qquad c = C_0 c^*, \qquad \bar{c} = C_0 \bar{c}^*, \tag{4.1}$$

where C_0 is defined in (3.5); again we drop the superscript stars for clarity.

(a) A semi-infinite slug of solute

First we consider the situation in which the solute initially takes the form of a semi-infinite slug of uniform concentration c_0 in $x \leq 0$, where c_0 is a constant, *i.e.* $c = c_0$ if $x \leq 0$ and $c = 0$ if $x > 0$. In his pioneering paper, Taylor [4] considered advection of such a slug in Poiseuille flow in a pipe

of circular cross-section, for which he showed that the mean concentration $\overline{c}$ is piecewise linear in the distance x down the pipe, specifically $\overline{c}=c_0$ for $x<0$, $\overline{c}=c_0[1-(x/u_{\max}t)]$ for $0\le x\le u_{\max}t$, and $\overline{c}=0$ for $x>u_{\max}t$. Note that there is nothing generic about this piecewise-linear dependence of $\overline{c}$ on x. For example, the corresponding calculation for two-dimensional Poiseuille flow yields $\overline{c}=c_0[1-(x/u_{\max}t)]^{1/2}$ for $0\le x\le u_{\max}t$, *i.e.* a square root dependence on x. However, the "self-similar" dependence on x and t in the combination x/t is generic for this problem.

For rivulet flow, with $C_0=c_0$, the (dimensionless) solution for c at time t is simply $c=1$ if $x\le ut$ and $c=0$ if $x>ut$, the slug having a "front" at $x=ut$, which is planar at $t=0$ but is curved for $t>0$; of course, since there is no slip at the substrate, the "base" of the front at $x=0$, $z=0$ remains stationary for all t. From (3.4), $\overline{c}$ at any station x and time t is the fraction of the cross-sectional area for which $u(y,z)\ge x/t$, which is of the self-similar form[1]

$$\overline{c}=\begin{cases}1 & \text{if } x<u_{\min}t,\\ f\left(\dfrac{x}{u_{\mathrm{m}}t}\right) & \text{if } u_{\min}t\le x\le u_{\max}t,\\ 0 & \text{if } x>u_{\max}t,\end{cases} \tag{4.2}$$

where u_{m} is defined by $u_{\mathrm{m}}=u_{\max}-u_{\min}$ (>0), and the function f, which is determined by (3.4), satisfies $0\le f(x/u_{\mathrm{m}}t)\le 1$, with $f(u_{\max}/u_{\mathrm{m}})=0$ and $f(u_{\min}/u_{\mathrm{m}})=1$.

Figure 2 shows the solution (4.2) for $\overline{c}$ in a rivulet on a vertical substrate plotted as a function of x for several values of τ at time $t=1$, with $a=1$ and $\beta=1$, illustrating clearly the advective effects of the flow for both positive and negative values of τ. (Note that because of the self-similar form of (4.2), plots of $\overline{c}$ at any other time $t>0$ will be the same as those in Fig. 2 except that in each case the x coordinate must be stretched by the amount $u_{\mathrm{m}}t$.) When $\tau\ge 0$ all of the solute is advected downwards, and therefore $c=1$ and hence $\overline{c}=1$ for $x\le 0$ for all t, which, in particular, explains why the curves for such cases in Fig. 2 all pass through $x=0$ and $\overline{c}=1$. Similarly, when $\tau\le -a\beta/2=-1/2$ all of the solute is advected upwards, and therefore $c=0$ and hence $\overline{c}=0$ for $x\ge 0$ for all t, which, in particular, explains why the curves for such cases in Fig. 2 all pass through $x=0$ and $\overline{c}=0$. Figure 2 also includes a curve for the critical value $\tau=\tau_{\mathrm{c}}=-2/7$ (shown dotted) for which the net advection is zero.

In principle, a complete list of the forms that the function f in (4.2) takes for different values of τ and α could be constructed, but it would be unwieldy, partly because, when $\tau<0$, several different forms of the velocity contour $u=x/t$ must be considered, each of which leads to a different form for f, and partly because it seems that, in general, the integral in (3.4) is not available in closed form when the substrate is not vertical (*i.e.* when $\alpha\ne\pi/2$), the free surface then having one of the non-parabolic profiles given in (A.1). However, in Appendix B we give explicit expressions for f in (4.2) in two cases in which $u\ge 0$ everywhere, namely flow on a vertical substrate with $\tau\ge 0$ and purely surface-shear-stress-driven flow; in both of these cases f decreases monotonically from the value 1 at $x=0$ to the value 0 at $x=u_{\max}t$.

(b) A finite slug of solute

Now we consider the situation in which the solute initially takes the form of a finite slug of uniform concentration c_0 in $0\le x\le\Delta$, where c_0 and Δ are constants, *i.e.* $c=c_0$ if $0\le x\le\Delta$ and $c=0$ if $x<0$ or $x>\Delta$. Again Taylor [4] considered advection of such a slug in Poiseuille flow in a pipe of circular cross-section, for which he again showed that $\overline{c}$ is piecewise linear in the distance x down the pipe.

For rivulet flow, with $C_0=c_0$ again, the (dimensionless) solution for c at time t is simply $c=0$ if $x\le ut$ or $x>ut+\Delta$ and $c=1$ if $ut<x\le ut+\Delta$, the slug in this case having both a front at

[1] The results (4.2) and (4.3)–(4.4) for advection in rivulet flow are, with appropriate re-interpretations of U and ℓ, also valid for advection of the corresponding slugs in unidirectional flow in a channel of arbitrary cross-section, and thus they generalise the results of Taylor [4] concerning advection in a pipe of circular cross-section.

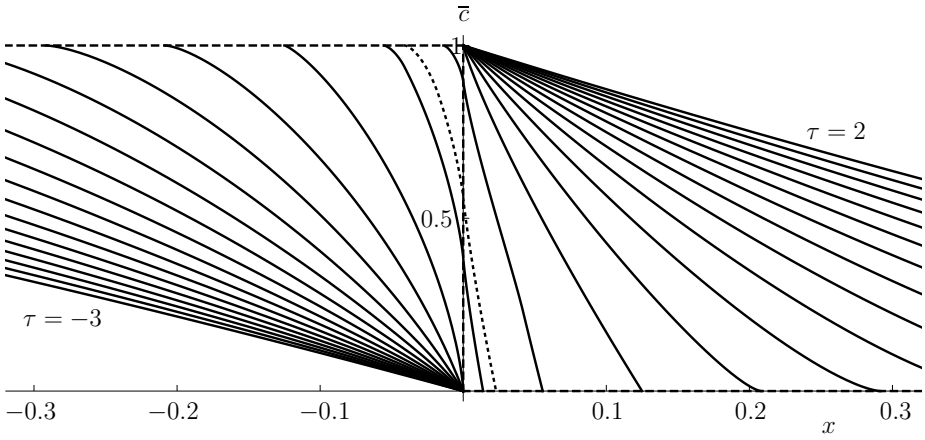

Figure 2. Mean concentration $\overline{c}$ in advection in a rivulet on a vertical substrate in the case when the solute initially takes the form of a semi-infinite slug of uniform concentration with $c = 1$ if $x \leq 0$ and $c = 0$ if $x > 0$ (shown dashed) given by (4.2) plotted as a function of x for $\tau = -3, -17/6, -8/3, \ldots, 2$ and $\tau = \tau_{\rm c} = -2/7$ (shown dotted) at time $t = 1$, with $a = 1$ and $\beta = 1$ in each case.

$x = ut + \Delta$ and a rear at $x = ut$. The solution for $\overline{c}$ at time t is given by

$$\overline{c} = \begin{cases} 0 & \text{if } x \leq u_{\rm min} t, \\ 1 - f\left(\dfrac{x}{u_{\rm m} t}\right) & \text{if } u_{\rm min} t < x \leq u_{\rm max} t, \\ 1 & \text{if } u_{\rm max} t < x \leq \Delta + u_{\rm min} t, \\ f\left(\dfrac{x - \Delta}{u_{\rm m} t}\right) & \text{if } \Delta + u_{\rm min} t < x \leq \Delta + u_{\rm max} t, \\ 0 & \text{if } x > \Delta + u_{\rm max} t \end{cases} \tag{4.3}$$

when $t \leq \Delta/u_{\rm m}$ (that is, up to the instant when the point of the rear of the slug at which the velocity is a maximum and the point of the front of the slug at which the velocity is a minimum first reach the same x value), and by

$$\overline{c} = \begin{cases} 0 & \text{if } x \leq u_{\rm min} t, \\ 1 - f\left(\dfrac{x}{u_{\rm m} t}\right) & \text{if } u_{\rm min} t < x \leq \Delta + u_{\rm min} t, \\ f\left(\dfrac{x - \Delta}{u_{\rm m} t}\right) - f\left(\dfrac{x}{u_{\rm m} t}\right) & \text{if } \Delta + u_{\rm min} t < x \leq u_{\rm max} t, \\ f\left(\dfrac{x - \Delta}{u_{\rm m} t}\right) & \text{if } u_{\rm max} t < x \leq \Delta + u_{\rm max} t, \\ 0 & \text{if } x > \Delta + u_{\rm max} t \end{cases} \tag{4.4}$$

when $t > \Delta/u_{\rm m}$, the function f in (4.3) and (4.4) being the same as that in (4.2).

Up to the instant $t = \Delta/u_{\rm m}$, $\overline{c}$ increases monotonically with x up to its maximum value 1, which is its value on a decreasing interval lying within $0 \leq x \leq \Delta$, and decreases monotonically with x to the right of this interval. At $t = \Delta/u_{\rm m}$ the interval has shrunk to a point at $x = (u_{\rm max}/u_{\rm m})\Delta$, and thereafter $\overline{c}$ satisfies $\overline{c} < 1$ everywhere, and can develop additional non-monotonic dependence on x beyond what it inherits in an obvious way from the initial distribution of c. Also $\overline{c}$ at $x = 0$ takes the constant value $1 - f(0)$ for $t \leq -\Delta/u_{\rm min}$, but (if $u_{\rm min} \neq 0$) decreases thereafter, whereas $\overline{c}$ at $x = \Delta$ takes the constant value $f(0)$ for $t \leq \Delta/u_{\rm max}$, but (if $u_{\rm max} \neq 0$) decreases thereafter.

Figure 3 shows three examples of the solution (4.3)–(4.4) for $\overline{c}$ in a rivulet on a vertical substrate plotted as a function of x/Δ at several times t, with $a = 1$ and $\beta = 1$, for (a) $\tau = -2/3$

(for which $u_{\max}=0$, $u_{\min}=-5/24$ and hence $u_{\rm m}=5/24$), (b) $\tau=-1/3$ (for which $u_{\max}=1/72$, $u_{\min}=-1/18$ and hence $u_{\rm m}=5/72$), and (c) $\tau=-1/6$ (for which $u_{\max}=1/18$, $u_{\min}=-1/72$ and hence $u_{\rm m}=5/72$). In particular, in Fig. 3(a) we have $\tau<-a\beta/2=-1/2$, and so all of the solute is advected upwards, whereas in Fig. 3(b) and (c) we have $-1/2=-a\beta/2<\tau<0$, and so both downwards and upwards advection occurs. In Fig. 3(c) (but not in Fig. 3(b)) non-monotonic dependence of $\overline{c}$ on x of the kind mentioned earlier is evident in $x>\Delta$. All of the solutions shown in Figure 3 are for cases with $\tau<0$. Solutions for cases with $\tau\geq 0$, in which all of the solute is advected downwards, are somewhat similar to the reflection of Fig. 3(a) in the line $x=1/2$, and so are omitted for brevity.

5. Taylor–Aris dispersion of a passive solute in a rivulet

For times longer than those considered in Section 4, the effects of diffusion are not negligible, and the concentration c satisfies the general advection–diffusion equation (3.1). In the remainder of the present work we will be concerned with Taylor–Aris dispersion of the solute at sufficiently long times. In particular, we will obtain the general expression for the effective diffusivity $D_{\rm eff}$ in the present rivulet flow. For definiteness we consider a situation somewhat similar to that considered in Section 4(b), in which the solute initially takes the form of a finite slug in $0\leq x\leq\Delta$, where Δ is a constant, with $c=0$ if $x<0$ or $x>\Delta$, except that now we allow the initial concentration $c(x,y,z,0)$ to be nonuniform. We non-dimensionalise and scale variables as in (2.1), together with

$$x=Lx^*,\qquad t=\frac{L}{U}t^*,\qquad c=C_0c^*,\qquad D_{\rm eff}=DD^*_{\rm eff},\tag{5.1}$$

where L is a characteristic length scale in the x direction and the mean initial concentration C_0 now takes the form

$$C_0=\frac{1}{A\Delta}\int_0^{\Delta}\int_{-a}^{a}\int_0^{h}c(x,y,z,0)\,{\rm d}z\,{\rm d}y\,{\rm d}x.\tag{5.2}$$

Then, with the stars again dropped for clarity, the governing equation and boundary conditions for c become, without approximation,

$$\delta\,{\rm Pe}(c_t+uc_x)=\delta^2c_{xx}+\nabla^2c,\qquad \mathbf{n}\cdot\nabla c=0\quad\text{on}\quad z=0\quad\text{and}\quad z=h,\tag{5.3}$$

where $\delta=\ell/L$ is a longitudinal aspect ratio and Pe is a Péclet number, defined by ${\rm Pe}=U\ell/D$. The time scale over which Taylor–Aris dispersion of the solute takes place is such that the aspect ratio $\delta\ll 1$ is small.

As is well known (see, for example, Taylor [4,5], Aris [6] and the references cited in Section 1), in Taylor–Aris dispersion of a passive solute in, for example, steady unidirectional pressure-driven flow in a channel of arbitrary cross-section Ω, the problem (5.3) leads to an advection–diffusion equation for $\overline{c}$ at leading order in δ, namely, in dimensional terms,

$$\overline{c}_t+\overline{u}\,\overline{c}_x=D_{\rm eff}\,\overline{c}_{xx},\tag{5.4}$$

where the effective diffusivity $D_{\rm eff}$ is conventionally expressed in the form

$$D_{\rm eff}=D\left(1+\kappa_{\rm con}{\rm Pe}_{\rm con}^2\right),\qquad \kappa_{\rm con}=\frac{1}{A}\iint_{\Omega}\frac{\widetilde{u}}{\overline{u}}\,C_{1\,\rm con}\,{\rm d}S,\tag{5.5}$$

where ${\rm Pe}_{\rm con}=\overline{u}\mathcal{L}/D$ (with $\mathcal{L}$ denoting a typical diameter of Ω) is a Péclet number conventionally used in studies of Taylor–Aris dispersion, A denotes the area of Ω, $\widetilde{u}=u-\overline{u}$ is the varying part of u which, by definition, satisfies

$$\iint_{\Omega}\widetilde{u}\,{\rm d}S=0,\tag{5.6}$$

and the dimensionless quantity $C_{1\,\rm con}$ is the solution of the Neumann problem

$$\mathcal{L}^2\nabla^2C_{1\,\rm con}=-\frac{\widetilde{u}}{\overline{u}}\quad\text{in}\quad\Omega,\qquad \mathbf{n}\cdot\nabla C_{1\,\rm con}=0\quad\text{on}\quad\partial\Omega,\qquad \iint_{\Omega}C_{1\,\rm con}\,{\rm d}S=0.\tag{5.7}$$

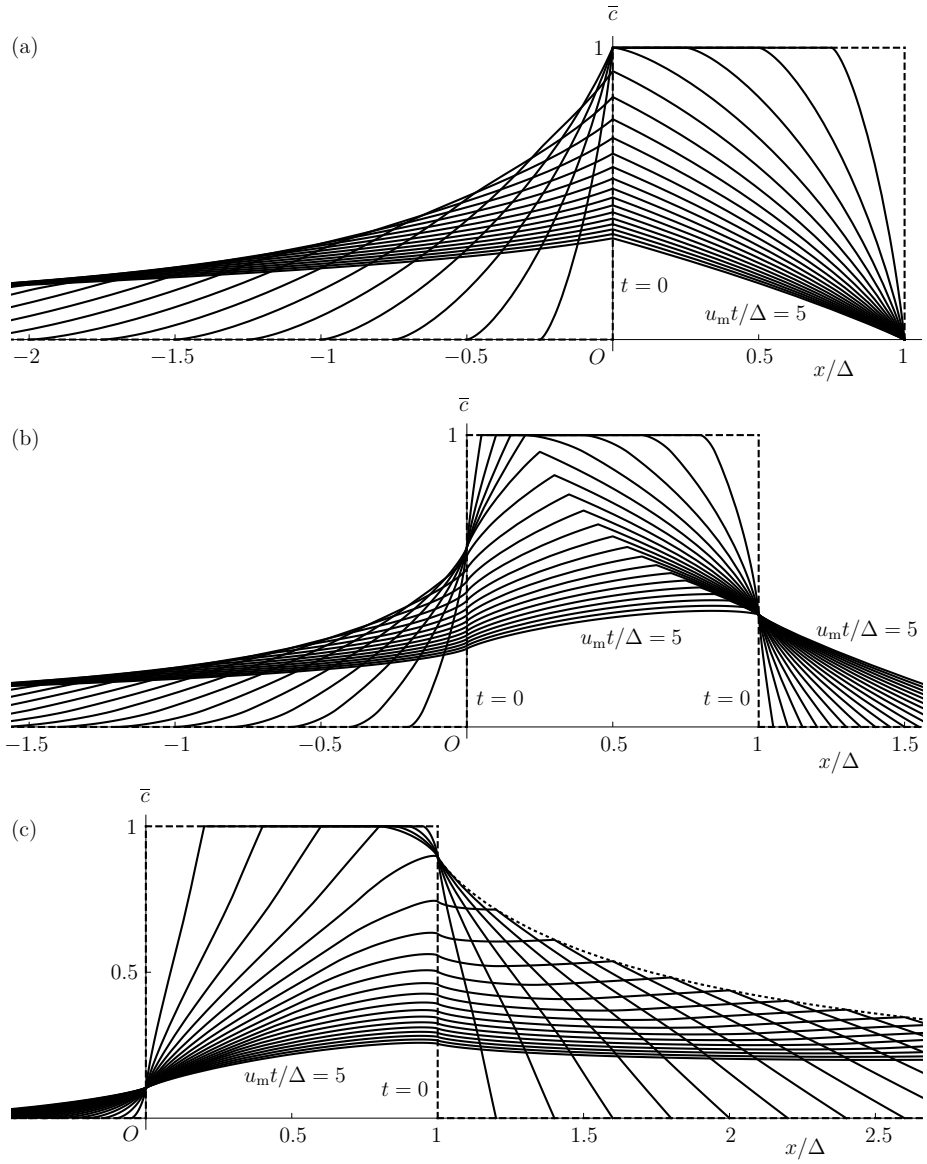

Figure 3. Mean concentration $\overline{c}$ in advection in a rivulet on a vertical substrate in cases when the solute initially takes the form of a finite slug of uniform concentration with $c=1$ if $0\le x\le \Delta$ and $c=0$ if $x<0$ or $x>\Delta$ (shown dashed) given by (4.3)–(4.4) plotted as a function of x/Δ at times t given by $u_{\rm m}t/\Delta=0,\,1/4,\,1/2,\,\ldots,\,5$ for (a) $\tau=-2/3$, (b) $\tau=-1/3$ and (c) $\tau=-1/6$, with $a=1$ and $\beta=1$ in each case (so that $u_{\rm m}=5/24,\,5/72$ and $5/72$, respectively). In part (c) the envelope of $\overline{c}$ in $x/\Delta\ge 1$ is shown dotted.

In Appendix C we show that an essentially identical result holds for Taylor–Aris dispersion of a passive solute in an, in general, non-thin, rivulet, namely

$$D_{\rm eff}=D\left(1+\kappa{\rm Pe}^2\right),\qquad \kappa=-\frac{1}{A}\iint_\Omega \frac{\widetilde{u}}{U}\,C_1\,{\rm d}S, \tag{5.8}$$

where C_1 is the solution of the Neumann problem

$$\ell^2\nabla^2 C_1=\frac{\widetilde{u}}{U}\quad\text{in}\quad\Omega,\qquad \mathbf{n}\cdot\nabla C_1=0\quad\text{on}\quad\partial\Omega,\qquad \iint_\Omega C_1\,{\rm d}S=0 \tag{5.9}$$

(again written in dimensional terms). We may, of course, choose to regard the quantities $\kappa_{\rm con}$, $\mathrm{Pe}_{\rm con}$ and $C_{1\,\rm con}$ as being related to κ, Pe and C_1 by

$$\kappa_{\rm con} = \left(\frac{U\ell}{\overline{u}\mathcal{L}}\right)^2 \kappa, \qquad \mathrm{Pe}_{\rm con} = \frac{\overline{u}\mathcal{L}}{U\ell}\mathrm{Pe}, \qquad C_{1\,\rm con} = -\frac{U\ell^2}{\overline{u}\mathcal{L}^2}C_1 \tag{5.10}$$

(so that $\kappa_{\rm con}\mathrm{Pe}_{\rm con}^2 = \kappa\,\mathrm{Pe}^2$). However, when we wish to compare values of $D_{\rm eff}$ in different rivulet flows with different values of τ, the formulation (5.5)–(5.7) is inconvenient, since both $\mathrm{Pe}_{\rm con}$ and $\kappa_{\rm con}$ depend on τ (via their dependence on $\overline{u}$), whereas in the formulation (5.8)–(5.9) used in the present study, Pe is independent of τ, and so the dependence of $D_{\rm eff}$ given by (5.8) on τ is isolated in just one parameter, namely κ. In addition, when τ takes the critical value $\tau = \tau_{\rm c}$ corresponding to no net flow, $\overline{u} = 0$, not only is the problem (5.7) for $C_{1\,\rm con}$ singular, but also $\mathrm{Pe}_{\rm con}$ is zero and $\kappa_{\rm con}$ is infinite (with $\kappa_{\rm con}\mathrm{Pe}_{\rm con}^2$ finite), meaning that in the conventional formulation it would be necessary to define $D_{\rm eff}$ via a limiting process; the present formulation avoids this complication. Moreover, if $\tau < \tau_{\rm c}$ then $\overline{u} < 0$ and so, slightly confusingly, $\mathrm{Pe}_{\rm con}$ is negative; again the present formulation, in which Pe is always positive, avoids this complication.

We now use the result (5.8)–(5.9) to analyse Taylor–Aris dispersion in a thin rivulet. As might be expected, the following development is somewhat similar to that of Guell *et al.* [21] and Ajdari *et al.* [24] for pressure-driven flow in a wide channel.[2]

(a) Taylor–Aris dispersion in a thin rivulet

For a thin rivulet, equation (5.9) gives, with the scalings (2.1) and (5.1),

$$C_{1yy} + \frac{1}{\epsilon^2}C_{1zz} = \epsilon^2(u - \overline{u}), \qquad C_{1z} = 0 \quad \text{on} \quad z = 0, \qquad C_{1z} = \epsilon^2 C_{1y}h' \quad \text{on} \quad z = h. \tag{5.11}$$

If we expand C_1 as

$$C_1 = \epsilon^2\left(C_{10} + \epsilon^2 C_{12} + \epsilon^4 C_{14} + \ldots\right), \tag{5.12}$$

then at leading order in ϵ we obtain

$$C_{10zz} = 0, \qquad C_{10z} = 0 \quad \text{on} \quad z = 0, \qquad C_{10z} = 0 \quad \text{on} \quad z = h, \tag{5.13}$$

so that $C_{10} = C_{10}(y)$. At first order in ϵ we obtain

$$C_{10}'' + C_{12zz} = u - \overline{u}, \qquad C_{12z} = 0 \quad \text{on} \quad z = 0, \qquad C_{12z} = C_{10}'h' \quad \text{on} \quad z = h. \tag{5.14}$$

Since the contact angle is non-zero, consistency of the boundary conditions in (5.14) at $y = \pm a$ requires that

$$C_{10}' = 0 \quad \text{at} \quad y = \pm a. \tag{5.15}$$

From (5.14) we have

$$C_{12} = \frac{\sin\alpha}{2}\left(\frac{hz^3}{3} - \frac{z^4}{12}\right) + \frac{\tau z^3}{6} - \left(\overline{u} + C_{10}''\right)\frac{z^2}{2} + k \tag{5.16}$$

for some arbitrary function $k = k(y)$, with

$$\left(hC_{10}'\right)' = R, \tag{5.17}$$

where for convenience we have written

$$R = R(y) = \frac{\sin\alpha\, h^3}{3} + \frac{\tau h^2}{2} - \overline{u}h. \tag{5.18}$$

Therefore

$$C_{10}' = \frac{1}{h}\int_{-a}^{y} R(\tilde{y})\,\mathrm{d}\tilde{y}, \tag{5.19}$$

[2] Note that there is a minor typographical error in equation (7) of Ajdari *et al.* [24], namely a missing opening square bracket before the second integral sign.

and hence

$$C_{10} = \int_{-a}^{y} \frac{1}{h(\hat{y})} \int_{-a}^{\hat{y}} R(\tilde{y})\, \mathrm{d}\tilde{y}\, \mathrm{d}\hat{y}, \tag{5.20}$$

the latter being correct up to an irrelevant additive constant.

Then taking the leading order terms in ϵ in equation (5.8) yields our main result concerning Taylor–Aris dispersion in a thin rivulet, namely that the general expression for the effective diffusivity D_{eff} takes the form

$$D_{\mathrm{eff}} = 1 + \kappa_0 \mathrm{Pe}^2, \tag{5.21}$$

in which $\mathrm{Pe} = U\ell/D$, and the coefficient κ_0 is given by

$$\kappa_0 = \frac{1}{A}\int_{-a}^{a} hC_{10}'^2\, \mathrm{d}y = \frac{1}{A}\int_{-a}^{a} \frac{1}{h}\left(\int_{-a}^{y} R(\tilde{y})\, \mathrm{d}\tilde{y}\right)^2 \mathrm{d}y, \tag{5.22}$$

or, more explicitly, by

$$\kappa_0 = \frac{1}{A^3}\int_{-a}^{a} \frac{1}{h(y)}\left\{\int_{-a}^{y} \frac{\sin\alpha}{3}\left[I_1 h(\tilde{y})^3 - I_3 h(\tilde{y})\right] + \frac{\tau}{2}\left[I_1 h(\tilde{y})^2 - I_2 h(\tilde{y})\right] \mathrm{d}\tilde{y}\right\}^2 \mathrm{d}y. \tag{5.23}$$

Note that, despite the fact that $h(\pm a) = 0$, the integral in (5.23) is convergent.

Since h (given explicitly by (A.1) in Appendix A) depends on α in a non-trivial way, the dependence of κ_0 in (5.23) on α is, in general, rather complicated. On the other hand, for a given value of α, if a and β are prescribed (in which case h is determined explicitly) then κ_0 is simply quadratic in τ. However, if Q is one of the prescribed quantities, along with either a or β (in which case h depends on τ via the flux relation (2.7)), then the dependence of κ_0 on τ is rather more complicated. These points may be understood more readily in the special case of a rivulet on a vertical substrate, which we discuss in detail in Section 5(b) below.

(b) Taylor–Aris dispersion in a thin rivulet on a vertical substrate

In the special case of a rivulet on a vertical substrate, in which h is given by (2.9), equation (5.20) gives

$$C_{10} = \frac{h_{\mathrm{m}}\left(a^2 - y^2\right)^2\left[20h_{\mathrm{m}}y^2 - 7a^2(8h_{\mathrm{m}} + 9\tau)\right]}{2520a^4}, \tag{5.24}$$

and (5.23) leads to an explicit expression for κ_0, namely

$$\kappa_0 = \frac{\beta^2 a^4\left(13388\beta^2a^2 + 57876a\beta\tau + 63063\tau^2\right)}{331080750}, \tag{5.25}$$

the interpretation of which depends on which two of the three quantities a, β and Q are prescribed, and on the prescribed value of τ, as we now describe.

(i) Purely gravity-driven flow

In the case $\tau = 0$ equation (5.25) yields $\kappa_0 = \kappa_{\mathrm{GD}}$ for dispersion in purely gravity-driven flow, where

$$\kappa_{\mathrm{GD}} = \frac{6694a^6\beta^4}{165540375} \simeq 4.0437 \times 10^{-5} a^6\beta^4, \tag{5.26}$$

which, when written in the form

$$\kappa_{\mathrm{GD}} = \frac{3347a^2\overline{u}^2}{270270} \simeq 0.0124a^2\overline{u}^2, \tag{5.27}$$

where $\overline{u} = 2a^2\beta^2/35$, can be recognised as being identical to the result for dispersion in pressure-driven flow in a wide channel of parabolic cross-section obtained by Ajdari *et al.* [24]. Since $Q =$

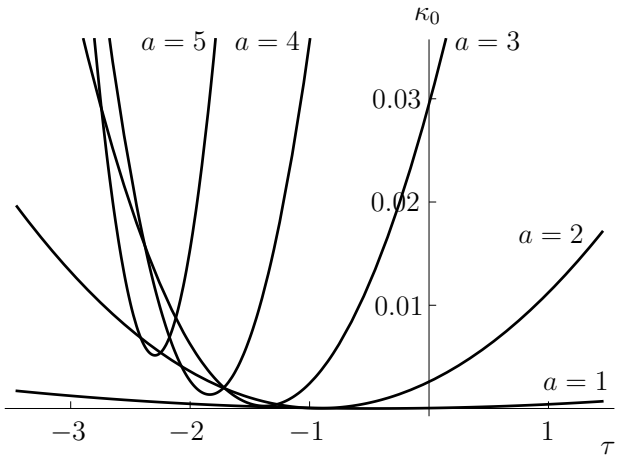

Figure 4. The coefficient κ_0 given by (5.25) plotted as a function of τ for a thin rivulet on a vertical substrate driven by both gravity and a surface shear stress τ, with prescribed a and β. The curves correspond to $a=1$ (lowest), 2, 3, 4 and 5 (highest), with $\beta=1$ in each case. (Note that, despite appearances, the curves do not touch the τ axis, that is, κ_0 is strictly positive.)

$4a^4\beta^3/105$ in this case, equation (5.26), which gives the most useful form of κ_0 if a and β are prescribed, may alternatively be written in the equivalent forms

$$\kappa_{\rm GD}=\frac{3347}{60060}\left(\frac{Q^3}{105\beta}\right)^{1/2}\simeq 0.0054\left(\frac{Q^3}{\beta}\right)^{1/2},\qquad \kappa_{\rm GD}=\frac{3347}{30030}\left(\frac{aQ^2}{210}\right)^{2/3}\simeq 0.0032(aQ^2)^{2/3}, \tag{5.28}$$

which are more useful if either β and Q are prescribed or a and Q are prescribed, respectively.

(ii) Purely surface-shear-stress-driven flow

In the limit $|\tau|\to\infty$ equation (5.25) yields κ_0, re-scaled as $\kappa_0=\tau^2\kappa_{\rm SD}$, for dispersion in purely shear-stress-driven flow, namely

$$\kappa_{\rm SD}=\frac{a^4\beta^2}{5250}\simeq 0.0002a^4\beta^2, \tag{5.29}$$

or equivalently

$$\kappa_{\rm SD}=\frac{a^2\widehat{\overline{u}}^2}{210}\simeq 0.0048a^2\widehat{\overline{u}}^2, \tag{5.30}$$

in which $\widehat{\overline{u}}=\overline{u}/\tau\to a\beta/5$. From (2.11), equation (5.29), which gives the most useful form of κ_0 if a and β are prescribed, may alternatively be rewritten in the equivalent forms

$$\kappa'_{\rm SD}=\frac{1}{140}\left(\frac{\sqrt{3}Q^2}{5\sqrt{2}\beta}\right)^{2/3}\simeq 0.0028\left(\frac{Q^2}{\beta}\right)^{2/3},\qquad \kappa''_{\rm SD}=\frac{aQ}{700}\simeq 0.0014aQ, \tag{5.31}$$

in which κ_0 has been re-scaled as $\kappa_0=\tau^{2/3}\kappa'_{\rm SD}$ and $\kappa_0=\tau\kappa''_{\rm SD}$, respectively, and which are more useful if either β and Q are prescribed or a and Q are prescribed, respectively.

(iii) A rivulet with prescribed a and β

If a and β are prescribed then, as previously mentioned, κ_0 in (5.25) is simply quadratic in τ. Figure 4 shows κ_0 given by (5.25) plotted as a function of τ for a range of values of a, with $\beta=1$; note that whereas a and β are constants on each curve, Q varies along the curves. The minimum value of κ_0 on a given curve is $\kappa_0=8a^4\beta^4/24279255\simeq 3.2950\times 10^{-7}a^4\beta^4$, occurring when $\tau=-106a\beta/231\simeq -0.4589a\beta$, and corresponding to $Q=-16a^4\beta^3/693\simeq -0.0231a^4\beta^3$;

for given values of a and β, values of κ_0 below this minimum are not achievable for any τ. Note also that two different values of τ, and hence two rivulets with different fluxes Q (but with the same values of a and β), can be associated with the same value of κ_0; for example, when $a=2$ and $\beta=1$, the value $\kappa_0=0.01$ is attained with $\tau\simeq-2.7273$ (for which $Q\simeq-2.2996$) and with $\tau\simeq0.8918$ (for which $Q\simeq1.5607$).

(iv) A rivulet with prescribed β and Q

If β and Q are prescribed then (2.9), (2.11) and (5.25) give κ_0 parametrically as a function of τ (with parameter a) in the form

$$\tau=\frac{15Q}{2a^3\beta^2}-\frac{2a\beta}{7},\qquad \kappa_0=\frac{8a^6\beta^4}{1324323}+\frac{4Qa^2\beta}{8085}+\frac{3Q^2}{280a^2\beta^2}. \tag{5.32}$$

In particular, κ_0 has branches satisfying

$$\kappa_0=\frac{1}{140}\left(\frac{3Q^4\tau^2}{50\beta^2}\right)^{1/3}+\frac{31}{2695}\left(\frac{Q^5}{60\beta\tau^2}\right)^{1/3}+O\left(\frac{1}{\tau}\right)\to\infty \tag{5.33}$$

in the limits $\tau\to\pm\infty$ (corresponding to $a\to0^+$), and a branch in $\tau<0$ satisfying

$$\kappa_0=\frac{343\tau^6}{30888\beta^2}+\frac{38Q\tau^2}{2145\beta}+O(\tau)\to\infty \tag{5.34}$$

in the limit $\tau\to-\infty$ (corresponding to $a\to+\infty$). In the special case $Q=0$ (which, for a nontrivial flow, is possible only for $\tau<0$), κ_0 is simply given by

$$\kappa_0=\frac{343\tau^6}{30888\beta^2}\simeq0.0111\left(\frac{\tau^3}{\beta}\right)^2\quad\text{for}\quad\tau<0. \tag{5.35}$$

Figure 5 shows κ_0 given by (5.32) plotted as a function of τ for a range of values of Q, together with the asymptotic results (5.33)–(5.34), with $\beta=1$ in each case. Note that whereas β and Q are constants on each curve in Fig. 5, a varies along the curves.

When $Q>0$ there is a unique value of κ_0 for each value of τ, but when Q satisfies $Q_{\min}<Q<0$, where $Q_{\min}=-3087\tau^4/5120\beta$, there are two values of κ_0 for each value of $\tau<0$. The latter non-uniqueness arises because, as Wilson and Duffy [33] describe, when $\tau<0$ there are two possible values of a (and hence two possible rivulets, a narrower one and a wider one) that correspond to such a value of Q; these two rivulets are associated with the smaller and larger values of κ_0, respectively. As Wilson and Duffy [33] also show, there is no rivulet solution when Q satisfies $Q<Q_{\min}$, or equivalently, when $\tau>\tau_{\max}$, where $\tau_{\max}=-(-5120\beta Q/3087)^{1/4}$ for $Q<0$; this is consistent with the fact that the curves for $Q<0$ in Fig. 5 lie entirely in $\tau\le\tau_{\max}$.

As Fig. 5 shows, κ_0 again has a minimum as a function of τ, namely

$$\kappa_0=\frac{1}{1155}\left(\frac{2\left(11518+217\sqrt{2821}\sigma\right)Q^3}{1365\beta}\right)^{1/2}\simeq0.0050\left(\frac{Q^3}{\beta}\right)^{1/2}\quad\text{or}\quad0.0001\left(-\frac{Q^3}{\beta}\right)^{1/2}, \tag{5.36}$$

when

$$\tau=\sigma\left(\frac{2\left(32874353\sqrt{2821}\sigma-1662451778\right)\beta Q}{3471933465}\right)^{1/4}\simeq0.4685\left(\beta Q\right)^{1/4}\quad\text{or}\quad-1.1837\left(-\beta Q\right)^{1/4}, \tag{5.37}$$

corresponding to

$$a=\left(\frac{21\left(\sqrt{2821}\sigma-26\right)Q}{40\beta^3}\right)^{1/4}\simeq1.9424\left(\frac{Q}{\beta^3}\right)^{1/4}\quad\text{or}\quad2.5386\left(-\frac{Q}{\beta^3}\right)^{1/4}, \tag{5.38}$$

where we have written $\sigma=\mathrm{sgn}(Q)=\pm1$, and the decimal approximations are valid for $Q>0$ and $Q<0$, respectively. For given values of β and Q, values of κ_0 below this minimum are not

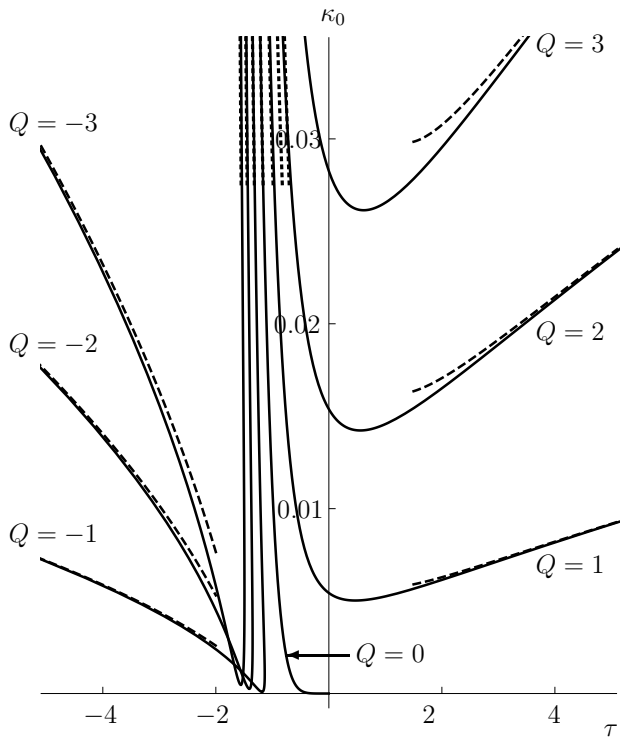

Figure 5. The coefficient κ_0 given by (5.32) plotted as a function of τ for a thin rivulet on a vertical substrate driven by both gravity and a surface shear stress τ, with prescribed β and Q. The curves correspond to $Q=-3,\,-2,\,-1,\,\ldots,\,3$, with $\beta=1$ in each case. The dashed and dotted curves show the asymptotic results (5.33)–(5.34), respectively.

achievable for any τ; moreover, except when $Q=0$, any value of κ_0 above its minimum can be achieved with two different values of τ, and hence with two different rivulets.

(v) A rivulet with prescribed a and Q

If a and Q are prescribed then κ_0 is again given parametrically as a function of τ by (5.32), but is now parameterised by β (rather than by a). Qualitatively the behaviour in this case is somewhat similar to that in the case of prescribed β and Q described in Section 5(b)(iv). In particular, κ_0 has branches satisfying

$$\kappa_0=\frac{aQ\tau}{700}+\frac{73}{5390}\left(\frac{aQ^3}{30\tau}\right)^{1/2}+O\left(\frac{1}{\tau}\right)\to\infty \tag{5.39}$$

in the limits $\tau\to\pm\infty$ (corresponding to $\beta\to 0^+$), and a branch in $\tau<0$ satisfying

$$\kappa_0=\frac{7a^2\tau^4}{7722}-\frac{178aQ\tau}{45045}+O(1)\to\infty \tag{5.40}$$

in the limit $\tau\to-\infty$ (corresponding to $\beta\to+\infty$). In the special case $Q=0$, κ_0 is simply given by

$$\kappa_0=\frac{7a^2\tau^4}{7722}\simeq 0.0009\left(a\tau^2\right)^2\quad\text{for}\quad\tau<0. \tag{5.41}$$

Figure 6 shows κ_0 given by (5.32) plotted as a function of τ for a range of values of Q, together with the asymptotic results (5.39)–(5.40), with $a=1$ in each case. Note that whereas a and Q are constants on each curve in Fig. 6, β varies along the curves.

As in the case of prescribed β and Q described in Section 5(b)(iv), when $Q>0$ there is a unique value of κ_0 for each value of τ, but when Q satisfies $Q_{\min}<Q<0$, where now $Q_{\min}=98\tau^3a/405$,

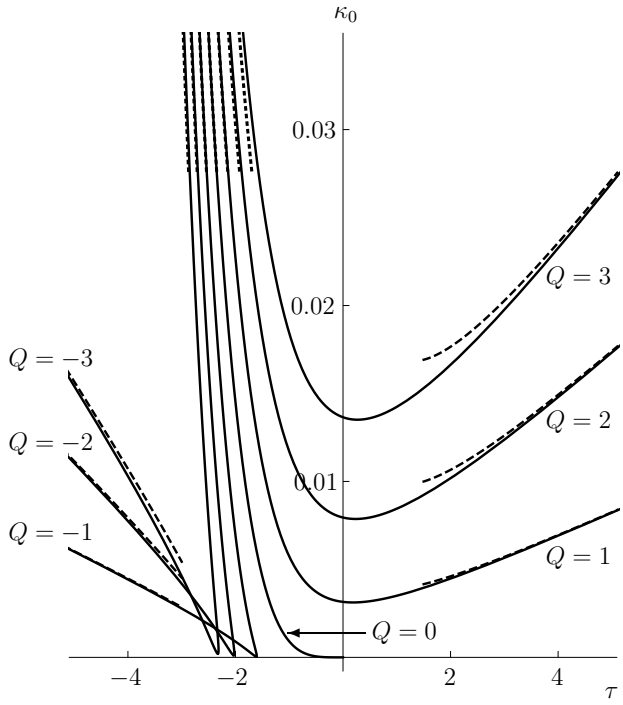

Figure 6. The coefficient κ_0 given by (5.32) plotted as a function of τ for a thin rivulet on a vertical substrate driven by both gravity and a surface shear stress τ, with prescribed a and Q. The curves correspond to $Q = -3, -2, -1, \ldots, 3$, with $a = 1$ in each case. The dashed and dotted curves show the asymptotic results (5.39)–(5.40), respectively.

there are two values of κ_0 for each value of $\tau < 0$, associated with two rivulets that have the same values of a and Q but different values of β. Also, the curves for $Q < 0$ in Fig. 6 lie entirely in $\tau \leq \tau_{\max}$, where now $\tau_{\max} = (405Q/98a)^{1/3}$.

As Fig. 6 shows, κ_0 again has a minimum as a function of τ, namely

$$\kappa_0 = \frac{3}{770}\left(\frac{\left(3279 + 82\sqrt{1599}\sigma\right)a^2Q^4}{14^2 \times 65}\right)^{1/3} \simeq 0.0031\left(aQ^2\right)^{2/3} \quad \text{or} \quad 5 \times 10^{-5}\left(aQ^2\right)^{2/3}, \tag{5.42}$$

when

$$\tau = \left(\frac{\left(4872223 - 121471\sqrt{1599}\sigma\right)Q}{77^2 \times 390a}\right)^{1/3} \simeq 0.1861\left(\frac{Q}{a}\right)^{1/3} \quad \text{or} \quad 1.6144\left(\frac{Q}{a}\right)^{1/3}, \tag{5.43}$$

corresponding to

$$\beta = \left(\frac{63\left(\sqrt{1599}\sigma - 13\right)Q}{80a^4}\right)^{1/3} \simeq 2.7700\left(\frac{Q}{a^4}\right)^{1/3} \quad \text{or} \quad -3.4685\left(\frac{Q}{a^4}\right)^{1/3}. \tag{5.44}$$

Once again, for given values of a and Q, values of κ_0 below this minimum are not achievable for any τ; moreover, except when $Q = 0$, any value of κ_0 above its minimum can again be achieved with two different values of τ, and hence with two different rivulets.

6. Summary and Conclusions

Motivated by the need for a better understanding of the transport of solutes in microfluidic flows with free surfaces, in the present contribution we analysed the advection and dispersion

of a passive solute in steady unidirectional flow of a thin uniform rivulet on an inclined planar substrate driven by gravity and/or a uniform longitudinal surface shear stress.

In Section 4 we described the short-time advection of both an initially semi-infinite and an initally finite slug of solute of uniform concentration. Examples were presented showing both downwards and upwards advection of solute, highlighting the fact that the dependence of $\overline{c}$ on x is not, in general, piecewise linear, and can develop additional non-monotonic dependence on x beyond what it inherits in an obvious way from the initial distribution of c.

In Section 5 we described the long-time Taylor–Aris dispersion of an initially finite slug of solute. In Appendix C we used the method of multiple scales to derive the formal expression for the effective diffusivity D_{eff} of a non-thin rivulet (or indeed any channel of arbitrary cross-section), from which in Section 5(a) we obtained our main result, namely the general expression for D_{eff} in a thin rivulet given by equations (5.21)–(5.23). In doing so, particular care was taken to formulate the problem in such a way as to avoid the complications that arise when $\overline{u} \leq 0$ (*i.e.* when $Q \leq 0$) when using the conventional formulation of the problem. In Section 5(b) we obtained the explicit expression for D_{eff} in the special case of a rivulet on a vertical substrate given by equations (5.21) and (5.25), and discussed in detail its different interpretations depending on which two of the three quantities a, β and Q are prescribed. In all three situations considered we found that, except in the special case of no net flow, $Q = 0$, the coefficient κ_0 always has a strictly positive global minimum as a function of τ (*i.e.* that D_{eff} is always strictly greater than D) and that any value of κ_0 above its minimum value can be achieved with two different values of τ (*i.e.* with two different rivulets).

As noted in Section 1, while the present work was primarily motivated by and described in the context of the dispersion of a solute, the present results also apply to the transport of heat with insulating boundary conditions and can readily be extended to other thermal boundary conditions, and so the present work is also relevant to the wide range of practical situations involving heat transfer in the presence of rivulets.

Data Accessibility. There are no datasets associated with the present work.

Competing Interests. We have no competing interests.

Authors' Contributions. B.R.D. and S.K.W. conceived of the study and drafted the manuscript. All three authors contributed to the mathematical calculations described in the present work and gave final approval for publication.

Funding. The first author (F.H.H.A.) was supported financially by the Ministry of Higher Education, Kingdom of Saudi Arabia and King Faisal University via an Academic Staff Training Fellowship. The third author (S.K.W.) was partially supported financially by the Leverhulme Trust via Research Fellowship RF-2013-355.

References

1. Stone HA, Stroock AD, Ajdari A. 2004 Engineering flows in small devices: Microfluidics toward a lab-on-a-chip, *Annu. Rev. Fluid Mech.* **36**, 381–411. (doi: 10.1146/annurev.fluid.36.050802.122124)
2. Darhuber AA, Troian SM. 2005 Principles of microfluidic actuation by modulation of surface stresses, Annu. Rev. Fluid Mech. **37**, 425–455. (doi: 10.1146/annurev.fluid.36.050802.122052)
3. Lee C-Y, Chang C-L, Wang Y-N, Fu L-M. 2011 Microfluidic mixing: A review, *Int. J. Mol. Sci.* **12**, 3263–3287. (doi: 10.3390/ijms12053263)
4. Taylor GI. 1953 Dispersion of soluble matter in solvent flowing slowly through a tube. *Proc. Roy. Soc. Lond. A* **219**, 186–203. (doi: 10.1098/rspa.1953.0139)
5. Taylor GI. 1954 Conditions under which dispersion of a solute in a stream of solvent can be used to measure molecular diffusion. *Proc. Roy. Soc. Lond. A* **225**, 473–477. (doi: 10.1098/rspa.1954.0216)
6. Aris R. 1956 On the dispersion of a solute in a fluid flowing through a tube. *Proc. Roy. Soc. Lond. A* **235**, 67–77. (doi: 10.1098/rspa.1956.0065)
7. Witelski T, Bowen M. 2015 *Methods of Mathematical Modelling*. New York: Springer.

8. Lungu EM, Moffatt HK. 1982 The effect of wall conductance on heat diffusion in duct flow. *J. Eng. Math.* **16**, 121–136. (doi: 10.1007/BF00042550)
9. Pagitsas M, Nadim A, Brenner H. 1986 Multiple time scale analysis of macrotransport processes. *Physica A* **135**, 533–550. (doi: 10.1016/0378-4371(86)90158-5)
10. Zhang J, Frigaard IA. 2006 Dispersion effects in the miscible displacement of two fluids in a duct of large aspect ratio. *J. Fluid Mech.* **549**, 225–251. (doi: 10.1017/S0022112005007846)
11. Mercer GN, Roberts AJ. 1990 A centre manifold description of contaminant dispersion in channels with varying flow properties. *SIAM J. Appl. Math.* **50**, 1547–1565. (doi: 10.1137/0150091)
12. Young WR, Jones S. 1991 Shear dispersion. *Phys. Fluids A* **3**, 1087–1101. (doi: 10.1063/1.858090)
13. Balakotaiah V, Chang H-C. 1995 Dispersion of chemical solutes in chromatographs and reactors. *Phil. Trans. Roy. Soc. Lond. A* **351**, 39–75. (doi: 10.1098/rsta.1995.0025)
14. Ratnakar RR, Balakotaiah V. 2011 Exact averaging of laminar dispersion. *Phys. Fluids* **23**, 023601. (doi: 10.1063/1.3555156)
15. Brenner H, Edwards DA. 1993 *Macrotransport Processes*. Oxford: Butterworth–Heinemann.
16. Dutta D, Leighton Jr DT. 2001 Dispersion reduction in pressure-driven flow through microetched channels. *Anal. Chem.* **73**, 504–513. (doi: 10.1021/ac0008385)
17. Dutta D, Ramachandran A, Leighton Jr, DT. 2006 Effect of channel geometry on solute dispersion in pressure-driven microfluidic systems. *Microfluid Nanofluid* **2**, 275–290. (doi: 10.1007/s10404-005-0070-7)
18. Dutta D. 2015 Hydrodynamic dispersion. In *Encyclopedia of Microfluidics and Nanofluidics* (edited by D. Li), pp 1313–1325. New York: Springer.
19. Doshi MR, Daiya PM, Gill WN. 1978 Three dimensional laminar dispersion in open and closed rectangular conduits. *Chem. Eng. Sci.* **33**, 795–804. (doi: 10.1016/0009-2509(78)85168-9)
20. Chatwin PC, Sullivan PJ. 1982 The effect of aspect ratio on longitudinal diffusivity in rectangular channels. *J. Fluid Mech.* **120**, 347–358. (doi: 10.1017/S0022112082002791)
21. Guell DC, Cox RG, Brenner H. 1987 Taylor dispersion in conduits of large aspect ratio. *Chem. Eng. Comm.* **58**, 231–244. (doi: 10.1080/00986448708911970)
22. Smith R. 1990 Two-dimensional shear dispersion for skewed flows in narrow gaps between moving surfaces. *J. Fluid Mech.* **214**, 211–228. (doi: 10.1017/S0022112090000118)
23. Smith R. 1990 Shear dispersion along a rotating axle in a closely fitting shaft. *J. Fluid Mech.* **219**, 647–658. (doi: 10.1017/S0022112090003135)
24. Ajdari A, Bontoux N, Stone HA. 2006 Hydrodynamic dispersion in shallow microchannels: the effect of cross-sectional shape. *Anal. Chem.* **78**, 387–392. (doi: 10.1021/ac0508651)
25. Darhuber AA, Chen JZ, Davis JM, Troian SM. 2004 A study of mixing in thermocapillary flows on micropatterned surfaces. *Phil. Trans. Roy. Soc. Lond. A* **362**, 1037–1058. (doi: 10.1098/rsta.2003.1361)
26. Kabov OA. 2010 Interfacial thermal fluid phenomena in thin liquid films. *Int. J. Emerging Multidisciplinary Fluid Sci.* **2**, 87–121. (doi: 10.1260/1756-8315.2.2-3.87)
27. Kabov OA, Bartashevich MV, Cheverda V. 2010 Rivulet flows in microchannels and minichannels. *Int. J. Emerging Multidisciplinary Fluid Sci.* **2**, 161–182. (doi: 10.1260/1756-8315.2.2-3.161)
28. Paterson C, Wilson SK, Duffy BR. 2013 Pinning, de-pinning and re-pinning of a slowly varying rivulet. *Euro. J. Mech. B/Fluids* **41**, 94–108. (doi: 10.1016/j.euromechflu.2013.02.006)
29. Young GW, Davis SH. 1987 Rivulet instabilities. *J. Fluid Mech.* **176**, 1–31. (doi: 10.1017/S0022112087000557)
30. Duffy BR, Moffatt HK. 1995 Flow of a viscous trickle on a slowly varying incline. *Chem. Eng. J.* **60**, 141–146. (doi: 10.1016/0923-0467(95)03030-1)
31. Myers TG, Liang HX, Wetton B. 2004 The stability and flow of a rivulet driven by interfacial shear and gravity. *Int. J. Non-Linear Mech.* **39**, 1239–1249. (doi: 10.1016/j.ijnonlinmec.2003.08.001)
32. Saber HH, El-Genk MS. 2004 On the breakup of a thin liquid film subject to interfacial shear. *J. Fluid Mech.* **500**, 113–133. (doi: 10.1017/S0022112003007080)
33. Wilson SK, Duffy BR. 2005 Unidirectional flow of a thin rivulet on a vertical substrate subject to a prescribed uniform shear stress at its free surface. *Phys. Fluids* **17**, 108105. (doi: 10.1063/1.2100987)
34. Sullivan JM, Wilson SK, Duffy BR. 2008 A thin rivulet of perfectly wetting fluid subject to a longitudinal surface shear stress. *Q. J. Mech. Appl. Math.* **61**, 25–61. (doi: 10.1093/qjmam/hbm023)

35. Benilov ES. 2009 On the stability of shallow rivulets. *J. Fluid Mech.* **636**, 455–474. (doi: 10.1017/S0022112009990802)
36. Tanasijczuk AJ, Perazzo CA, Gratton J. 2010 Navier–Stokes solutions for steady parallel-sided pendent rivulets. *Eur. J. Mech. B/Fluids* **29**, 465–471. (doi: 10.1016/j.euromechflu.2010.06.002)
37. Wilson SK, Sullivan JM, Duffy BR. 2011 The energetics of the breakup of a sheet and of a rivulet on a vertical substrate in the presence of a uniform surface shear stress. *J. Fluid Mech.* **674**, 281–306. (doi: 10.1017/S0022112010006518)
38. Herrada MA, Mohamed AS, Montanero JM, Gañán-Calvo AM. 2015 Stability of a rivulet flowing in a microchannel. *Int. J. Multiphase Flow* **69**, 1–7. (doi: 10.1016/j.ijmultiphaseflow.2014.10.012)
39. Bender CM, Orszag, SA. 1999 *Advanced Mathematical Methods for Scientists and Engineers I: Asymptotic Methods and Perturbation Theory*. New York: Springer.

A. The solution of equations (2.5)–(2.6) for h

In this Appendix we record the solution of (2.5)–(2.6) for the profile $h(y)$ of a thin uniform rivulet undergoing steady unidirectional flow on a planar substrate inclined at an angle α ($0 \le \alpha \le \pi$) to the horizontal, the flow being driven by gravity and/or a uniform longitudinal surface shear stress τ. We also provide explicit expressions for the quantities I_1, I_2 and I_3 defined in (2.8) and appearing in the expressions for Q and $\overline{u}$ given in (2.7).

The solution of (2.5) subject to (2.6) is

$$h = \beta \times \begin{cases} \dfrac{\cosh ma - \cosh my}{m \sinh ma} & \text{if} \quad 0 \le \alpha < \dfrac{\pi}{2}, \\ \dfrac{a^2 - y^2}{2a} & \text{if} \quad \alpha = \dfrac{\pi}{2}, \\ \dfrac{\cos my - \cos ma}{m \sin ma} & \text{if} \quad \dfrac{\pi}{2} < \alpha \le \pi, \end{cases} \tag{A.1}$$

where we have introduced the notation $m = |\cos\alpha|$. Therefore the maximum thickness of the rivulet, $h_{\rm m} = h(0)$, is given by

$$h_{\rm m} = \frac{\beta}{m} \times \begin{cases} \tanh \dfrac{ma}{2} & \text{if} \quad 0 \le \alpha < \dfrac{\pi}{2}, \\ \dfrac{ma}{2} & \text{if} \quad \alpha = \dfrac{\pi}{2}, \\ \tan \dfrac{ma}{2} & \text{if} \quad \dfrac{\pi}{2} < \alpha \le \pi, \end{cases} \tag{A.2}$$

and the flux Q and mean velocity $\overline{u}$ are given by (2.7), in which the I_n defined in (2.8) are given by

$$I_1 = \frac{2\beta}{m^2} \times \begin{cases} ma \coth ma - 1 & \text{if} \quad 0 \le \alpha < \dfrac{\pi}{2}, \\ \dfrac{(ma)^2}{3} & \text{if} \quad \alpha = \dfrac{\pi}{2}, \\ 1 - ma \cot ma & \text{if} \quad \dfrac{\pi}{2} < \alpha \le \pi, \end{cases} \tag{A.3}$$

$$I_2 = \frac{\beta^2}{m^3} \times \begin{cases} 3ma \coth^2 ma - 3 \coth ma - ma & \text{if} \quad 0 \le \alpha < \dfrac{\pi}{2}, \\ \dfrac{4(ma)^3}{15} & \text{if} \quad \alpha = \dfrac{\pi}{2}, \\ 3ma \cot^3 ma - 3 \cot ma + ma & \text{if} \quad \dfrac{\pi}{2} < \alpha \le \pi, \end{cases} \tag{A.4}$$

$$I_3 = \frac{\beta^3}{3m^4} \times \begin{cases} 15ma\coth^3 ma - 15\coth^2 ma - 9ma\coth ma + 4 & \text{if} \quad 0 \le \alpha < \dfrac{\pi}{2}, \\ \dfrac{12(ma)^4}{35} & \text{if} \quad \alpha = \dfrac{\pi}{2}, \\ -15ma\cot^3 ma + 15\cot^2 ma - 9ma\cot ma + 4 & \text{if} \quad \dfrac{\pi}{2} < \alpha \le \pi. \end{cases} \tag{A.5}$$

In all of the above, if $0 \le \alpha \le \pi/2$ then $ma \ge 0$, whereas if $\pi/2 < \alpha \le \pi$ then $0 < ma \le \pi$. Note that the expressions for I_2 and I_3 were first given in these compact forms by Sullivan *et al.* [34] and Duffy and Moffatt [30], respectively.

B. Advection in a rivulet: two cases in which $u \ge 0$ everywhere

In this Appendix we obtain explicit expressions for the function f appearing in equations (4.2), (4.3)–(4.4) in two cases in which $u \ge 0$ everywhere, namely flow on a vertical substrate with $\tau \ge 0$ and purely surface-shear-stress-driven flow.

(a) Flow on a vertical substrate with $\tau \ge 0$

In the case of flow on a vertical substrate (*i.e.* when $\alpha = \pi/2$) and $\tau \ge 0$, in which case $u_{\rm m} = u_{\max} = h_{\rm m}(h_{\rm m} + 2\tau)/2$ and $u_{\min} = 0$, the condition $u \ge x/t$ for any value of x satisfying $0 \le x \le u_{\max} t$ is equivalent to the condition $H \le z \le h$, where $z = H$ $(0 \le H \le h)$ denotes the curve on which $u = x/t$, so that from (2.4)

$$H = h + \tau - \left[(h+\tau)^2 - \frac{2x}{t}\right]^{1/2}. \tag{B.1}$$

The curve (B.1) intersects the free surface $z = h$ at $y = \pm b$, where

$$b = a\left[1 + \frac{\tau}{h_{\rm m}} - \left(\frac{\tau^2}{h_{\rm m}^2} + \frac{2x}{h_{\rm m}^2 t}\right)^{1/2}\right]^{1/2}, \tag{B.2}$$

and the function f in (4.2) is given by

$$f = \int_{-b}^{b}\int_{H}^{h} \mathrm{d}z\,\mathrm{d}y = \int_{-b}^{b} (h - H)\,\mathrm{d}y, \tag{B.3}$$

which leads to

$$\begin{aligned} f = \left[1 + \frac{\tau}{h_{\rm m}} + \left(\frac{2x}{h_{\rm m}^2 t}\right)^{1/2}\right]^{1/2} \left[\left(1 + \frac{\tau}{h_{\rm m}}\right) E(\phi|m) - \left(\frac{2x}{h_{\rm m}^2 t}\right)^{1/2} F(\phi|m)\right] \\ - \frac{\tau}{h_{\rm m}}\left[1 + \frac{\tau}{h_{\rm m}} - \left(\frac{\tau^2}{h_{\rm m}^2} + \frac{2x}{h_{\rm m}^2 t}\right)^{1/2}\right]^{1/2}, \end{aligned} \tag{B.4}$$

where F and E denote incomplete elliptic integrals of the first and second kinds, respectively, with

$$\phi = \sin^{-1}\left[\left(\frac{1 + \frac{\tau}{h_{\rm m}} - \left(\frac{\tau^2}{h_{\rm m}^2} + \frac{2x}{h_{\rm m}^2 t}\right)^{1/2}}{1 + \frac{\tau}{h_{\rm m}} - \left(\frac{2x}{h_{\rm m}^2 t}\right)^{1/2}}\right)^{1/2}\right], \qquad m = \frac{1 + \frac{\tau}{h_{\rm m}} - \left(\frac{2x}{h_{\rm m}^2 t}\right)^{1/2}}{1 + \frac{\tau}{h_{\rm m}} + \left(\frac{2x}{h_{\rm m}^2 t}\right)^{1/2}}. \tag{B.5}$$

In particular, in the case of purely gravity-driven flow ($\tau = 0$) equations (B.4)–(B.5) reduce to

$$f = \left[1 + \left(\frac{2x}{h_{\rm m}^2 t}\right)^{1/2}\right]^{1/2}\left[E(m) - \left(\frac{2x}{h_{\rm m}^2 t}\right)^{1/2} K(m)\right], \qquad m = \frac{1 - \left(\frac{2x}{h_{\rm m}^2 t}\right)^{1/2}}{1 + \left(\frac{2x}{h_{\rm m}^2 t}\right)^{1/2}}, \tag{B.6}$$

where K and E denote complete elliptic integrals of the first and second kinds, respectively. From (B.4) we have

$$\frac{\partial f}{\partial x} = -\frac{3F(\phi|m)}{2h_{\rm m}^2 t\left[1+\dfrac{\tau}{h_{\rm m}}+\left(\dfrac{2x}{h_{\rm m}^2 t}\right)^{1/2}\right]^{1/2}}, \tag{B.7}$$

showing that $\partial f/\partial x < 0$ for $0 \le x \le u_{\max} t$, that is, f decreases monotonically with x. In Fig. 2 the curves for $\tau \ge 1/6$ and the curve for $\tau = 0$ correspond to (B.4) and (B.6), respectively.

(b) Purely surface-shear-stress-driven flow

In the case of purely shear-stress-driven flow, for which $u = \tau z$, $u_{\rm m} = u_{\max} = \tau h_{\rm m}$ and $u_{\min} = 0$, a similar analysis to that outlined in Section B(a) reveals that the corresponding forms for H and b are $H = x/\tau t$ and

$$b = \begin{cases} \dfrac{1}{m}\cosh^{-1}\left(\cosh ma - \dfrac{(\cosh ma - 1)x}{\tau h_{\rm m} t}\right) & \text{if} \quad 0 \le \alpha < \dfrac{\pi}{2}, \\ a\left(1 - \dfrac{x}{\tau h_{\rm m} t}\right)^{1/2} & \text{if} \quad \alpha = \dfrac{\pi}{2}, \\ \dfrac{1}{m}\cos^{-1}\left(\cos ma + \dfrac{(1-\cos ma)x}{\tau h_{\rm m} t}\right) & \text{if} \quad \dfrac{\pi}{2} < \alpha \le \pi, \end{cases} \tag{B.8}$$

where m is again defined by $m = |\cos\alpha|$. Then from (3.4) the function f in (4.2) is given by

$$f = \begin{cases} \dfrac{1}{ma\cosh ma - \sinh ma}\left(mb\cosh ma - \sinh mb - (\cosh ma - 1)\dfrac{mbx}{\tau h_{\rm m} t}\right) & \text{if} \quad 0 \le \alpha < \dfrac{\pi}{2}, \\ \left(1 - \dfrac{x}{\tau h_{\rm m} t}\right)^{3/2} & \text{if} \quad \alpha = \dfrac{\pi}{2}, \\ \dfrac{1}{ma\cos ma - \sin ma}\left(mb\cos ma - \sin mb + (1-\cos ma)\dfrac{mbx}{\tau h_{\rm m} t}\right) & \text{if} \quad \dfrac{\pi}{2} < \alpha \le \pi \end{cases} \tag{B.9}$$

for $0 \le x \le \tau h_{\rm m} t$. From (B.9) we have

$$\frac{\partial f}{\partial x} = -\frac{1}{\tau h_{\rm m} t}\begin{cases} \dfrac{mb(\cosh ma - 1)}{ma\cosh ma - \sinh ma} & \text{if} \quad 0 \le \alpha < \dfrac{\pi}{2}, \\ \dfrac{3}{2}\left(1 - \dfrac{x}{\tau h_{\rm m} t}\right)^{1/2} & \text{if} \quad \alpha = \dfrac{\pi}{2}, \\ \dfrac{mb(1-\cos ma)}{\sin ma - ma\cos ma} & \text{if} \quad \dfrac{\pi}{2} < \alpha \le \pi, \end{cases} \tag{B.10}$$

showing again that $\partial f/\partial x < 0$ for $0 \le x \le u_{\max} t$, that is, f decreases monotonically with x.

C. Taylor–Aris dispersion in a non-thin rivulet

In this Appendix we use the method of multiple scales to derive from (5.3) the formal expression for the effective diffusivity $D_{\rm eff}$ of an, in general, *non-thin* rivulet, from which in Section 5 we will obtain our main result, namely the general expression for $D_{\rm eff}$ in a thin rivulet given by equations (5.21)–(5.23). In fact, the following analysis is valid not only for rivulet flow but for Taylor–Aris dispersion in steady unidirectional flow along *any* channel of arbitrary cross-section.

The time scale over which Taylor–Aris dispersion takes place is such that the aspect ratio $\delta \ll 1$ is small, and we seek the leading order behaviour of $D_{\rm eff}$ in the limit $\delta \to 0$ with ${\rm Pe} = O(1)$.

First, it is convenient to change to a frame moving with velocity $\overline{u}$; writing $\xi = x - \overline{u}\,t$ and $T = t$ we have

$$\delta\,{\rm Pe}(c_T + \widetilde{u}\,c_\xi) = \delta^2 c_{\xi\xi} + \nabla^2 c, \qquad \mathbf{n}\cdot\nabla c = 0 \quad \text{on} \quad z = 0 \quad \text{and} \quad z = h, \tag{C.1}$$

where $\widetilde{u} = u - \overline{u}$.

We use a multiple-scales expansion (see, for example, Bender and Orszag [39]), with times T_n ($n = 0, 1, 2, \dots$) defined by $T_n = \delta^n T$, so that (C.1) gives

$$\delta \,\mathrm{Pe}\left(c_{T_0} + \delta c_{T_1} + \delta^2 c_{T_2} + \widetilde{u}\, c_\xi\right) = \delta^2 c_{\xi\xi} + \nabla^2 c + O(\delta^3). \tag{C.2}$$

We expand c as $c = c_0 + \delta c_1 + \delta^2 c_2 + O(\delta^3)$ with $c_n = c_n(\xi, y, z, T_0, T_1, \dots)$; then (C.2) leads to

$$\nabla^2 c_0 = 0, \tag{C.3}$$

$$\mathrm{Pe}\left(c_{0T_0} + \widetilde{u}\, c_{0\xi}\right) = \nabla^2 c_1, \tag{C.4}$$

$$\mathrm{Pe}\left(c_{1T_0} + c_{0T_1} + \widetilde{u}\, c_{1\xi}\right) = c_{0\xi\xi} + \nabla^2 c_2, \tag{C.5}$$

and so on. Also the boundary condition in (C.1) gives

$$\mathbf{n}\cdot\nabla c_n = 0 \quad \text{on} \quad z = 0 \quad \text{and} \quad z = h, \qquad n = 0, 1, 2, \dots. \tag{C.6}$$

Multiplying (C.3) by c_0, integrating over the cross-section of the rivulet, Ω, and using Green's theorem and (C.6) yields

$$\begin{aligned} 0 &= \iint_\Omega c_0 \nabla^2 c_0 \,\mathrm{d}S \\ &= \iint_\Omega \left[\nabla\cdot(c_0\nabla c_0) - (\nabla c_0 \cdot \nabla c_0)\right] \mathrm{d}S \\ &= \oint_{\partial\Omega} c_0 \nabla c_0 \cdot \mathbf{n}\,\mathrm{d}s - \iint_\Omega \left|\nabla c_0\right|^2 \mathrm{d}S \\ &= -\iint_\Omega \left|\nabla c_0\right|^2 \mathrm{d}S, \end{aligned} \tag{C.7}$$

where $\partial\Omega$ denotes the boundary of Ω (comprising the substrate $z = 0$ and the free surface $z = h$) and s denotes arc length along $\partial\Omega$. Therefore $\left|\nabla c_0\right|^2 = 0$, and so $c_{0y} = c_{0z} = 0$, showing that c_0 is independent of y and z.

Integration of (C.4) over Ω gives

$$\iint_\Omega \nabla^2 c_1 \,\mathrm{d}S = A\,\mathrm{Pe}\, c_{0T_0}. \tag{C.8}$$

Using Green's theorem and (C.6) with $n = 1$ we have

$$\iint_\Omega \nabla^2 c_1 \,\mathrm{d}S = \oint_{\partial\Omega} \nabla c_1 \cdot \mathbf{n}\,\mathrm{d}s = 0, \tag{C.9}$$

so that (C.8) gives $c_{0T_0} = 0$. We deduce that c_0 depends on $\xi, T_1, T_2, \dots$ only, and, from (C.4), that c_1 therefore satisfies

$$\nabla^2 c_1 = \mathrm{Pe}\,\widetilde{u}\, c_{0\xi}. \tag{C.10}$$

Defining $C_1 = C_1(\xi, y, z, T_0, T_1, \dots)$ by

$$c_1 = \mathrm{Pe}\, c_{0\xi} C_1, \tag{C.11}$$

C_1 satisfies the Neumann problem

$$\nabla^2 C_1 = \widetilde{u} \quad \text{in} \quad \Omega, \qquad \mathbf{n}\cdot\nabla C_1 = 0 \quad \text{on} \quad \partial\Omega. \tag{C.12}$$

Clearly C_1 is determined only up to an additive function of $\xi, T_0, T_1, \dots$, that is, if $C_1 = \phi_1(y, z)$ is one solution of (C.12) then so is $C_1 = \phi_1(y, z) + \psi_1(\xi, T_0, T_1, \dots)$, with ψ_1 arbitrary. It is convenient to choose ψ_1 to be minus the cross-sectional mean of ϕ_1 (which is a constant, independent of $\xi, y, z, T_0, T_1, \dots$); then C_1 depends on y and z only, and

$$\iint_\Omega C_1 \,\mathrm{d}S = 0, \tag{C.13}$$

with which (C.12) determines C_1 uniquely.

Integration of (C.5) over Ω gives

$$\mathrm{Pe}\left(\iint_\Omega c_{1T_0}\,\mathrm{d}S + Ac_{0T_1} + \iint_\Omega \widetilde{u}\,c_{1\xi}\,\mathrm{d}S\right) = Ac_{0\xi\xi} + \iint_\Omega \nabla^2 c_2\,\mathrm{d}S, \tag{C.14}$$

which, using Green's theorem and (C.11), may be written in the form

$$\mathrm{Pe}\left[\mathrm{Pe}\,c_{0\xi}\frac{\partial}{\partial T_0}\iint_\Omega C_1\,\mathrm{d}S + Ac_{0T_1} + \mathrm{Pe}\,\frac{\partial}{\partial\xi}\left(c_{0\xi}\iint_\Omega \widetilde{u}\,C_1\,\mathrm{d}S\right)\right] = Ac_{0\xi\xi} + \oint_{\partial\Omega}\nabla c_2\cdot\mathbf{n}\,\mathrm{d}s. \tag{C.15}$$

Using (C.6) and (C.13) then gives

$$\mathrm{Pe}\,Ac_{0T_1} + \mathrm{Pe}^2 c_{0\xi\xi}\iint_\Omega \widetilde{u}\,C_1\,\mathrm{d}S = Ac_{0\xi\xi}, \tag{C.16}$$

leading to the formal expression for the effective diffusivity D_{eff}, namely

$$c_{0T_1} = \frac{D_{\mathrm{eff}}}{\mathrm{Pe}}c_{0\xi\xi}, \qquad D_{\mathrm{eff}} = 1+\kappa\mathrm{Pe}^2, \qquad \kappa = -\frac{1}{A}\iint_\Omega \widetilde{u}\,C_1\,\mathrm{d}S, \tag{C.17}$$

where C_1 is the solution of (C.12)–(C.13).

Moreover, using Green's theorem and (C.12) we have

$$\begin{aligned}\iint_\Omega \widetilde{u}\,C_1\,\mathrm{d}S &= \iint_\Omega C_1\nabla^2 C_1\,\mathrm{d}S\\ &= \iint_\Omega\left[\nabla\cdot(C_1\nabla C_1) - (\nabla C_1\cdot\nabla C_1)\right]\mathrm{d}S\\ &= \oint_{\partial\Omega} C_1\nabla C_1\cdot\mathbf{n}\,\mathrm{d}s - \iint_\Omega\left|\nabla C_1\right|^2\mathrm{d}S\\ &= -\iint_\Omega\left|\nabla C_1\right|^2\mathrm{d}S,\end{aligned} \tag{C.18}$$

so that D_{eff} in (C.17) may be written in the alternative form

$$D_{\mathrm{eff}} = 1+\kappa\mathrm{Pe}^2, \qquad \kappa = \frac{1}{A}\iint_\Omega\left|\nabla C_1\right|^2\mathrm{d}S, \tag{C.19}$$

which shows, in particular, that $D_{\mathrm{eff}} > 1$.

In dimensional terms the formal expression (C.17) is

$$c_{0t} + \overline{u}c_{0x} = D_{\mathrm{eff}}\,c_{0xx}, \qquad D_{\mathrm{eff}} = D\left(1+\kappa\mathrm{Pe}^2\right), \qquad \kappa = -\frac{1}{A}\iint_\Omega \frac{\widetilde{u}}{U}\,C_1\,\mathrm{d}S, \qquad \mathrm{Pe} = \frac{U\ell}{D}, \tag{C.20}$$

showing that at leading order in δ the solute moves with the mean velocity $\overline{u}$ and diffuses with an effective diffusivity D_{eff}. Note also that $\overline{c} = c_0$ at leading order in δ, and so the first equation in (C.20) may alternatively be written in the form $\overline{c}_t + \overline{u}\,\overline{c}_x = D_{\mathrm{eff}}\,\overline{c}_{xx}$, which is equation (5.4).